Chemical Physics Letters 710 (2018) 207–214

Contents lists available at ScienceDirect

Chemical Physics Letters

journal homepage: www.elsevier.com/locate/cplett

Research paper

Vibrational, energetic-dynamical and dissociation properties of water clusters in static electric fields: Non-equilibrium molecular-dynamics insights

Somendra Nath Chakraborty[a,*], Niall J. English[b]

[a] Department of Chemistry, Sikkim University, Gangtok, India
[b] School of Chemical and Bioprocess Engineering, University College Dublin, Belfield, Dublin 4, Ireland

HIGHLIGHTS

- Water clusters (2, 6, 12 and 20) are simulated under additional forces of varying magnitude of 0.1–25 % of the total force.
- The original cluster breaks immediately within 1 ns and alternate arrangements are taken up even at low fields.
- The librational peaks are most effected with 20 water clusters being most effected, they are suppressed with time.

ARTICLE INFO

Keywords:
Water cluster
Hydrogen bond
Molecular dyanmics
Electic field

ABSTRACT

Water clusters are hydrogen bonded molecular assembly of water molecules. They have been extensively studied using experiments, ab initio calculations and molecular simulations. The molecular arrangement of water in water cluster provide significant insights into behavior of water in bulk, confinement and close to surfaces. Here molecular dynamics simulations of TIP4P/2005 water clusters are performed in weak electrid fields. These fields introduce additional forces of varying magnitude 0.1–25% of forces existing in without-field water clusters. Autocorrelation functions of distance, energy and velocities are analysed. Molecular arrangements in water clusters does not disintegrate under additional forces.

1. Introduction

Hydrogen bonding is generally relatively weak, essentially Coulombic interaction between a hydrogen atom bonded covalently to an electronegative atom (such as oxygen) and another electronegative atom. Hydrogen bonds are directional, their strength typically ≈1–10 kcal/mol range. In the condensed phase, hydrogen-bond vibrations, dynamics and stability govern the properties of liquid water, ice and clathrate hydrates [1–4], whilst this holds also for gas-phase clusters of water molecules [5–8]; indeed, these properties have been investigated extensively using both theoretical and experimental techniques [9,10]. For instance, using ab initio molecular dynamics (MD), Kühne and Khallliulin have studied the asymmetry of co-existing weaker and stronger hydrogen bonds in liquid water [11], serving to rationalise SAXS measurements and the controversial two-liquid model of water as an explanation of thermodynamic anomalies [12]. Hydrogen-bond orientational mechanisms have been studied explicitly by MD in terms of a jump mechanism explaining water reorientation via hydrogen-bond cleavage and molecular reorientation occurring concertedly [13]. A wide range of hydrogen-bonding energetic and vibtrational properties has been studied using quantum-chemistry methods, density functional theory (DFT) and empirical-potential methods for a whole suite of water clusters, ranging from dimers to $(H_2O)_{20}$ [5–8], with the latter $(H_2O)_{20}$ case not dissimilar to pentagonal dodecahdral 5^{12} cages in clathrate hydrates [4]; indeed, Yoo et al. have studied further $(H_2O)_{24}$ clusters, and their incorporation into clathrate-hydrate lattices via proton-network optimisation, in view of their similarity to tetrakaidecharal cages [14]. In particular, Ref. [6] discusses with acuity and insight the importance and subtleties of anharmonicity in vibrational properties in determining the relative energies of water clusters.

The influence of electric fields on water and aqueous systems is crucial in underpinning our knowledge of electric-field effects on wider systems, e.g., in biology, and molecular simulation has much to offer in terms of mechanistic understading [15]. Electric fields have been applied to water cluster, and many of the fascinating physico-chemical

* Corresponding author.
E-mail address: snchakraborty@cus.ac.in (S.N. Chakraborty).

https://doi.org/10.1016/j.cplett.2018.08.061
Received 14 May 2018; Accepted 24 August 2018
Available online 31 August 2018

properties been dissected by molecular simulation. Indeed, due to the inherent difficulty in defining time in optimising structures between states to locate putative transition paths, static fields have been applied to eigenvector-following/basin-hopping optimisation methods by James et al., and applied to the study of change in structure of water clusters (without PBC) based on both increasing field strength and the number of water molecules in each type of cluster, using model potentials [16]. It was found that structures became extended in more intense fields, echoing the findings of dipole stretching in MC of flexible structures [20–23]. Choi et al. carried out aperiodic DFT-based geometry optimisation of a series of water clusters increasing in size in a static electric field, and concluded that clusters open to form a linear chain in the direction of the field, due to dipole alignment [24]; this is broadly in line with the findings of James et al. [16] from transition-path sampling using model potentials. There has been much interest in static-field effects on water clusters, chiefly from a structure-perturbation perspective [20,24–33] using either geometry-optimisation, Monte Carlo, transition-path sampling or MD with force fields [20,25,26,31], DFT [24,27–30,32] and CCSD(T) [33]. The threshold for altering the structure of water clusters is generally higher in static fields than for the bulk liquid, although this depends on the size of the cluster. At lower-intensity fields, less than around 0.3–0.5 V/Å, hydrogen-bond structural reorganisation takes place with physical effects of (partial) dipolar alignment with stretching along the field direction in some cases, whilst above this intensity, chemical characteristics of the atoms and molecules can be altered. Similarly, the physical response of water clusters to static fields has been studied in terms of dipolar alignment, and this polarisation response quantified at various field intensities [20,25–33].

In any event, despite this encouraging progress in the past decade or so of water-cluster research in external electric fields, an open question in the water-cluster literature relates as to the dynamical effect of static electric fields on vibrational properties as well as those of stabilising hydrogen bonds across a wide range of intact clusters, as probed by finite-temperature MD. In addition a more rigorous establishment of approximate field intensities required to rupture, and rearrange permanently, the underlying stabilising hydrogen-bonding arrangements of a broad gamut of clusters over sub-microsecond timescales is needed. In the latter case, assessing applied-field strengths of those present intrinsically is important, so as to study these trends in field-intensity thresholds and survival times as function of external-to-intrinsic field-intensity ratios. Here we perform molcular dynamics simulations of 2, 6, 12 and 20 water clusters under the influence of low (0.01, 0.1 and 0.25 V/nm) and strong (0.5, 1.0, 1.5 and 2.0 V/nm) electric field. The relaxation behaviour of hydrogen bond distances, energies and velocities are understood and the survival times of hydrogen bonds as a function of electric field strength are obtained and analysed. Improving the overall understanding hydrogen-bonding arrangements in bulk water is of great interest to scientists. Hydrogen bonds, and their abilities to form various structures, result in different anomalous properties of water [34]. The hydrogen-bonding arrangement in the local neighbourhood of a water molecule holds the key towards understanding the behaviour of water. Water clusters are an important set of systems where local hydrogen-bonding arrangements can be investigated easily and understood. Water clusters under the influence of electric fields give us additional insights into understanding hydrogen-bond patterns, and their snapping tendencies. In previous simulations, asymmetry in hydrogen bonding [11], phase change [26] and electro-freezing of bulk water under the influence of electric fields, has been investigated [35]. The application of electric fields to water clusters has resulted in different hydrogen-bonding arrangements, and, as such, serves as a potent reminder of the importance of the entropic agent of field-induced dipole alignment. Indeed, this has been highlighted in the case of subtle differences in phase changes in nanoscale water clusters very recently [36]. In the present study, motivated by this background, we assess the structural changes of hydrogen bonding in water clusters under the influence of electric fields.

Table 1
Potential parameters used in the simulations.

Model	q	σ (nm)	ϵ/k_B (K)
TIP4P/2005	−1.1128	0.3159	93.20

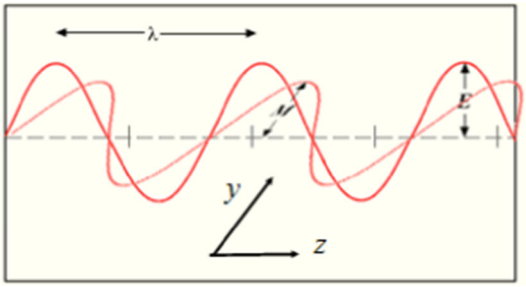

Fig. 1. Schematic model of plane-polarised e/m wave.

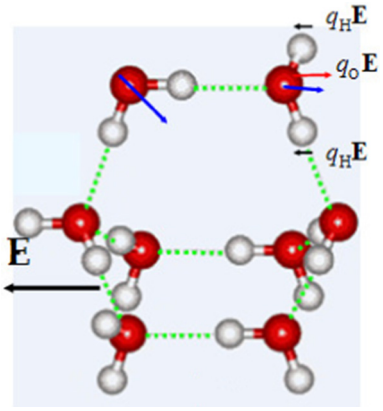

Fig. 2. lectric field/force vectors on a sample water-cluster system. The external electric force vector **E** is shown by the heavy black arrow, whilst the electric-force vectors exerted on the oxygen and hydrogen atoms are shown by lighter red and black arrows, respectively, with blue dipole vectors shown for comparison. Hydrogen bonds are depicted by dotted green lines. (For interpretation of the references to colour in this figure legend, the reader is referred to the web version of this article.)

Table 2
Average forces on water Oxygen under zero field.

Cluster size	Force (pN)
2	1005
6	2279
12	2551
20	2449

Table 3
External-field forces on water Oxygen under varying fields.

Electric field intensities (V/nm)	Forces (pN)
0.01	2.01
0.10	18.3
0.25	44.3
0.50	88.4
1.00	177
1.50	266
2.00	354

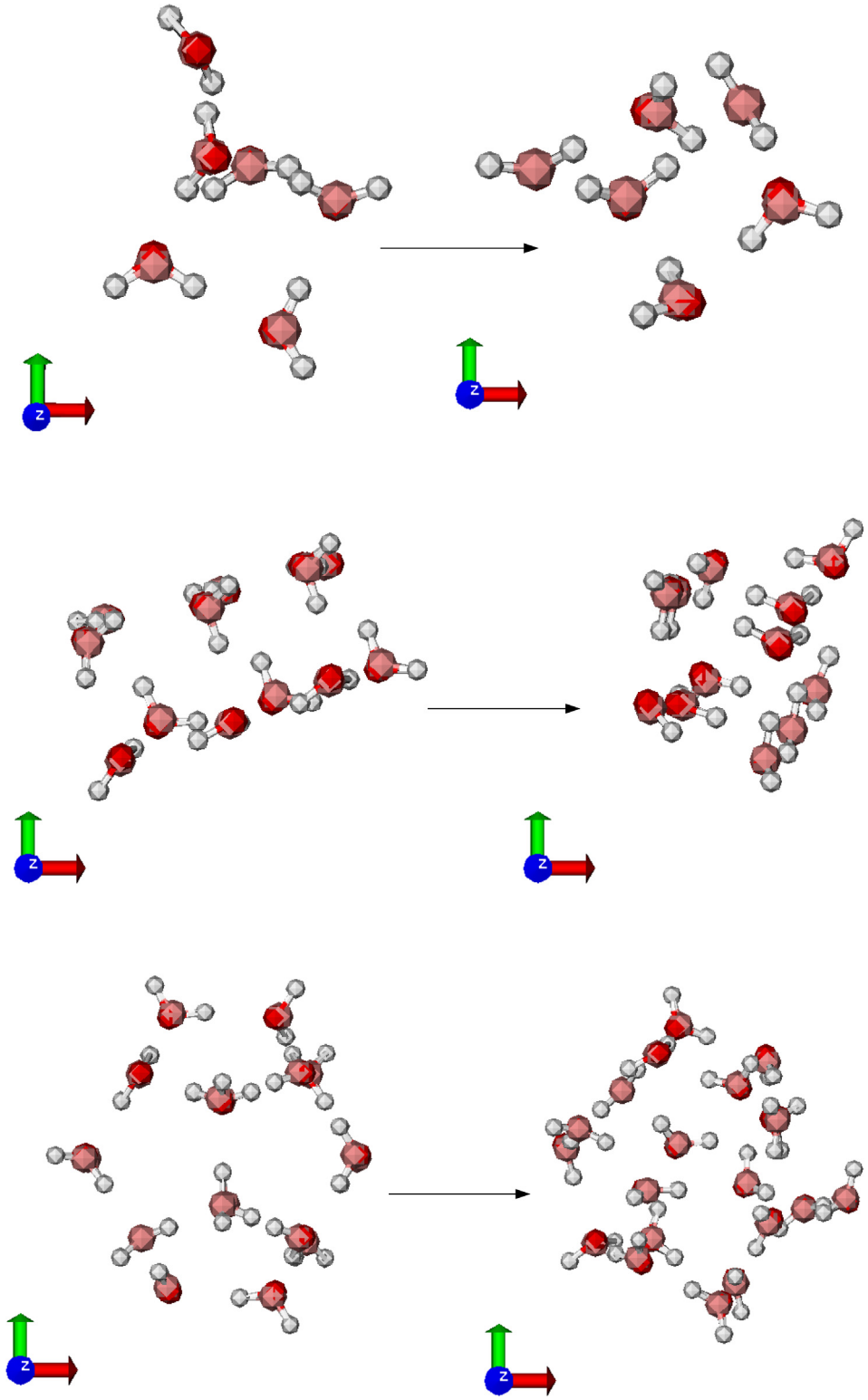

Fig. 3. Snapshots show 6, 12 and 20 water cluster at the begining and end of 200 ps run.

2. Computational details

Molecular Dynamics simulations of water clusters containing 2, 6, 12 and 20 water molecules were performed under the influence of electric fields. For simulating the 2, 6 and 12 molecules water clusters, globally optimised structures of these clusters were obtained from Cambridge Cluster Database [39]. Choice of initial cluster configuration is an essential input for water cluster simulations. Different initial structures generate different energy minimum. Global minimum for water cluster is the ideal choice for initiating the simulations. Here optimised structures of water clusters at zero field is chosen for all the simulations. These structures may not tbe the optimised structures for different values of electric field, nevertheless they are good approximations to the initial structures to start the simulations. The 20 molecule water cluster simulated is a 5^{12} water cage observed in crystal structure of sI and sII hydrate. All water molecules in these clusters

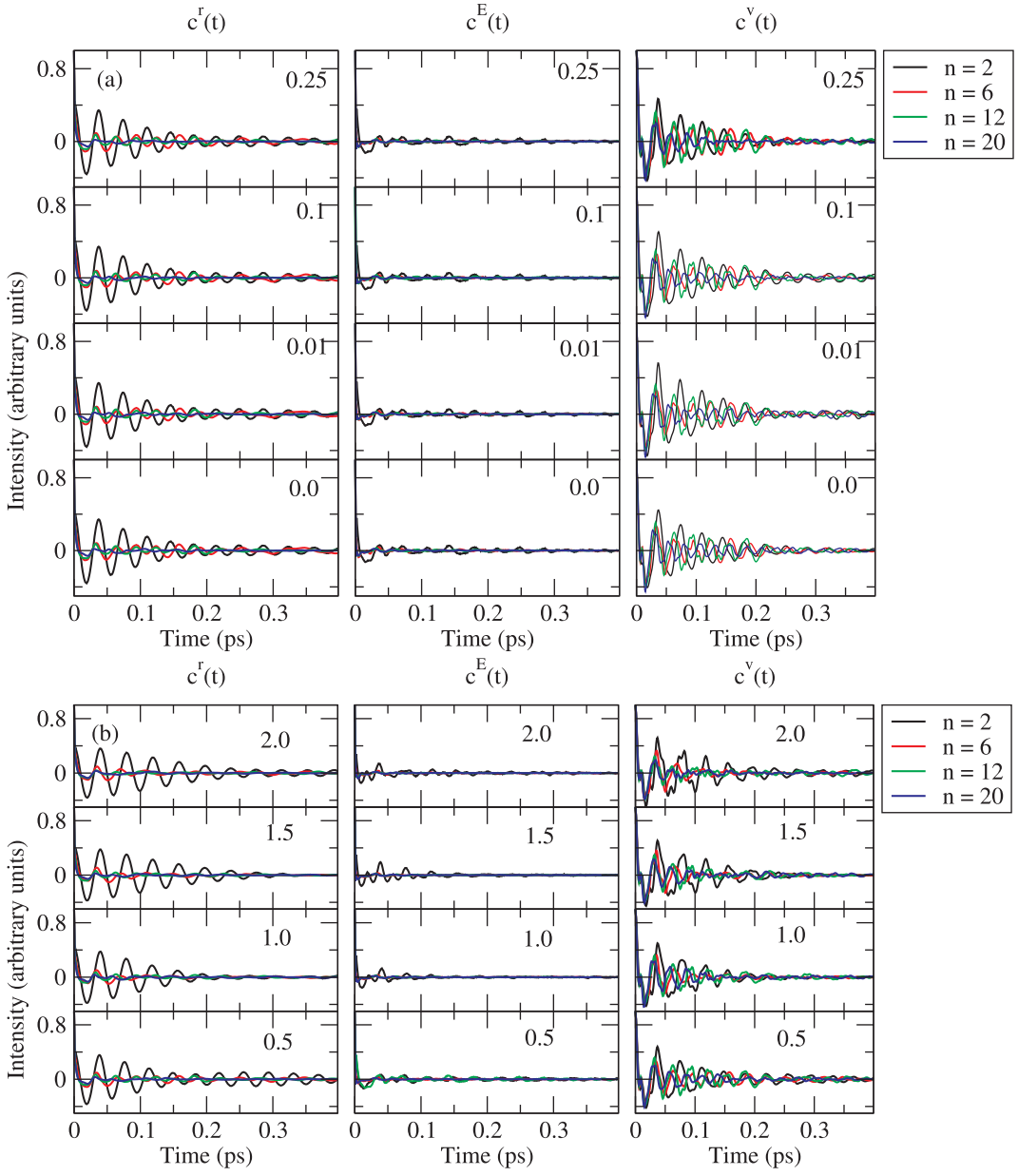

Fig. 4. (a) Autocorrelation functions at 0 ns at 0.0, 0.01, 0.1 and 0.25 V/nm. (b) Autocorrelation functions at 0 ns at 0.5, 1.0, 1.5 and 2.0 V/nm.

were modeled using TIP4P/2005 potential. The details of the potential model are presented in Table 1 [37]. In the four-site TIP4P/2005 model, positive charges are located on the hydrogen atoms, with the negative charge of 1.1128e not located on the oxygen atom but 0.1546 Åtoward the hydrogens along the HOH angle bisector. The single LJ interaction site is again centered on the oxygen atom. The OH distance is 0.9572 Å, and the HOH angle is 104.52°. This model has provided good agreement with the experimental studies of liquid water [37]. TIP4P family of potentials has also been used earlier to study water clusters [16,17]. Lowest energy structures for TIP4P potentials under influence of electric field has been obtained earlier [31,16]. In another study melting of SPC/E water clusters was invetigated using MD simulations. Initial structures were chosen as fragments of cubic and hexagonal ice and water cluster sizes were varied from 8 to 40. Melting temperatures were found to be above 100 K for all these water clusters [18]. Here all the different sizes of water clusters were simulated at 0.0, 0.01, 0.1, 0.25, 0.5, 1.0, 1.5 and 2.0 V/nm. The electric field in all these cases were applied normal to the z axis. Here water clusters under additional forces of magnitudes 0.1–25% more than in no-field situations are used for the simulations. All the simulations were performed for 1 μs. Data was collected from 200 ps short runs at 0, 200, 400, 600 and 800 ns. Time step of 1 fs was used to perform the integration and verlet-leapfrog alogorithm was used for this. Since classical MD simulations were performed a finite temperature was required to obtain the dynamics of the cluster. A high temperture will evaporate the cluster and therefore a low temperature of 100 K was fixed for the simulations. Velocity-rescale was used at every 2 ps to maintain the temperature. Number of particles and temperature was fixed and GROMACS molecular dynammics package was used for the siulations. LINCS algorithm was used to constrain the angles and bonds in the water molecule [19]. For all systems, the Luzar-Chandler geometric hydrogen-bond recognition criteria (i.e., R_{OO} is < 3.5 Åand O-O-axis-to O-H-bond angle >150°) [3] were applied to identify hydrogen bonds per water molecule in each configuration. The interaction energy between the two water molecules involved in each hydrogen bond was computed (in terms of both Lennard-Jones contributions and all pairwise local Coulombic interactions between all charge sites). This defined each hydrogen bond's instantaneous (self-) energy, $E_i(t)$ while its

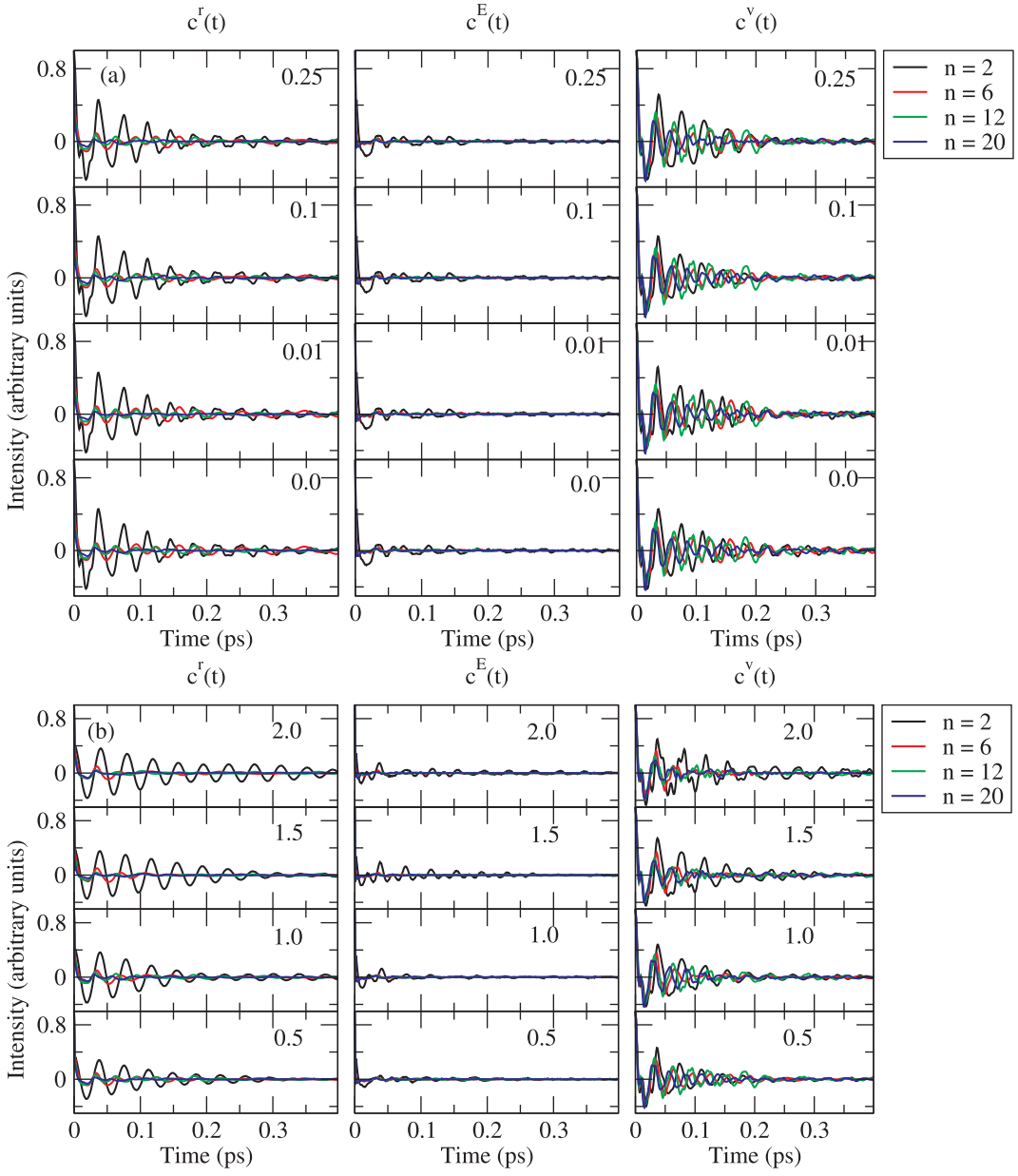

Fig. 5. (a) Autocorrelation functions at 800 ns at 0.0, 0.01, 0.1 and 0.25 V/nm. (b) Autocorrelation functions at 800 ns at 0.5, 1.0, 1.5 and 2.0 V/nm.

length at that instant was $r_i(t)$. Interaction energies between the two molecules involved in each hydrogen bond were used to determine that bonds self-energy. Normalised autocorrelation functions (ACF) of hydrogen-bond distance, energy and velocities time-derivatives by averaging over all the hydrogen bonds were obtained using -

$$c^{\alpha}(t) = \langle \dot{\alpha}_i(t)\dot{\alpha}_i(0)\rangle / \langle \dot{\alpha}_i(0)\dot{\alpha}_i(0)\rangle$$

where α = r, E or v. The use of time-derivatives, $\dot{\alpha}$ in the definition has the advantage of being acutely sensitive to temporal fluctutations (e.g. periodic ocillations or 'vibrations') in α, allowing this to be probed conveniently and straightforwardly via power spectra of the ACFs (i.e. their real-space Fourier transformations). Fig. 1 shows a schematic of a propagating electromagnetic wave and Fig. 2 shows the representations of the Electric field vector on a water-cluster.

3. Results and discussion

The autocorrelations and power spectra are analysed for all the water clusters, under varying electric fields. Electric fields exert additional forces on the water molecules. The forces acting on water molecules without electric fields are tabulated in Table 2. Table 3 shows the magitude of additional forces acting on the water molecules as a result of the external electric fields. The forces were calculated as the forces acting on the oxygen of the water molecules. The additional forces acting on 2 water clusters vary from 0.2% to 25% of the total forces in low and high electric fields respectively. Whereas the additional forces acting on 6, 12 and 20 water molecules vary from 0.1% to 12% of the total forces in low and high fields respectively. Snapshots in Fig. 3 shows the 6,12 and 20 water cluster under the influence of 2.0 V/nm electric field at the begining and end of 200 ps. It is observed that within 200 ps the initial structure of the water cluster is deformed. The 20 molecule water cage cluster completely deforms within the first 200 ps of the run. The ACFs and spectra is discussed in the following section.

3.1. Auto-correlation functions

The auto-correlation functions (ACF) of distances, energies and

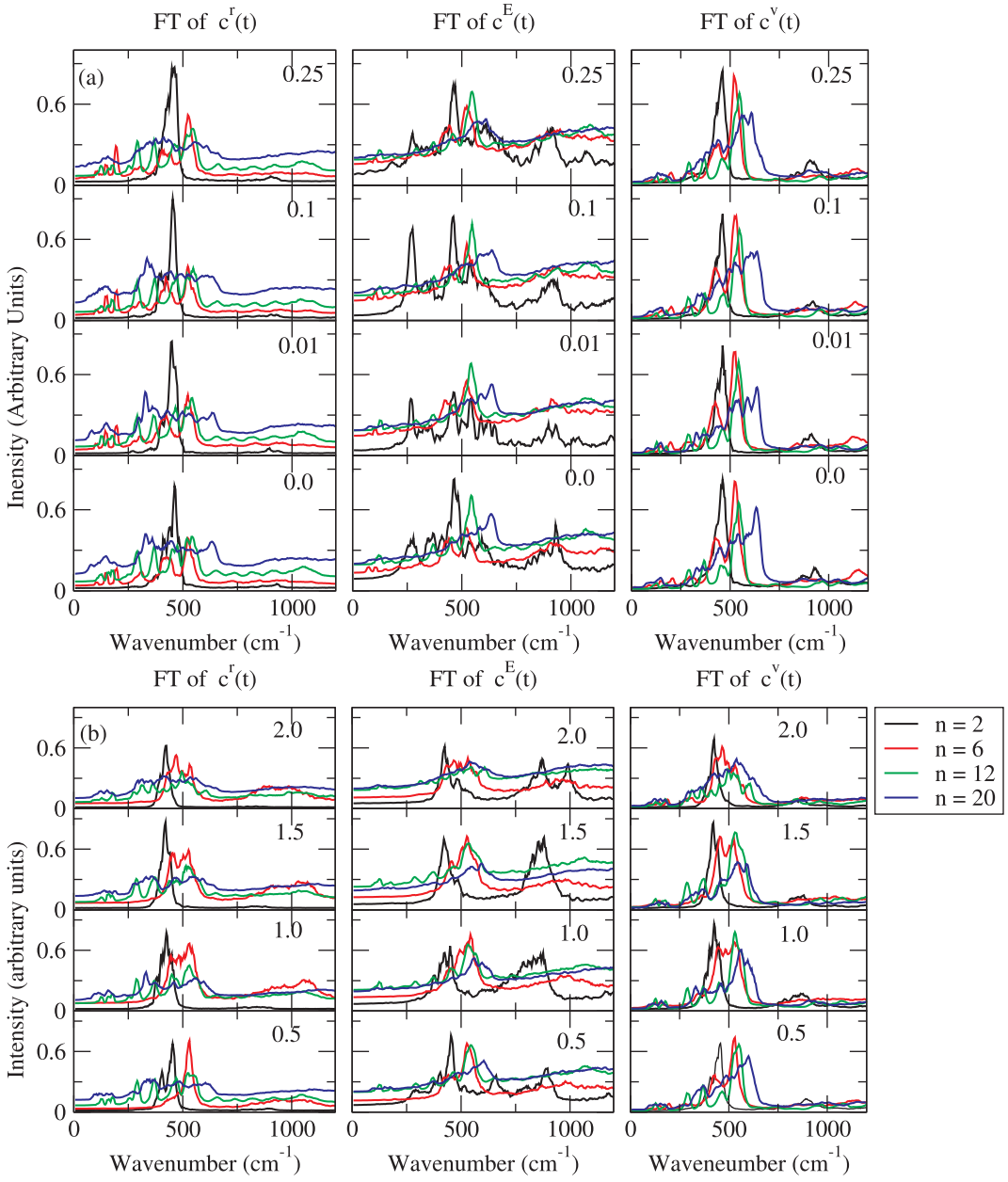

Fig. 6. (a) Fourier Transform of Autocorrelation functions at 0 ns at 0.0, 0.01, 0.1 and 0.25 V/nm. (b) Fourier Transform of Autocorrelation functions at 0 ns at 0.5, 1.0, 1.5 and 2.0 V/nm.

velocities at 0 and 800 ns are plotted in Figs. 4 and 5. ACFs at 200, 400 and 600 ns were obtained and provided in Supplementary Information. They were not significantly different from those at 0 ns. Auto-correlations of distances, energies and velocities are plotted for each value of electric field for every water cluster. Comparison of acf of distances, energies and velocities at 0 and 800 ns in Figs. 4 and 5 show that relaxation of quantities occur in the following decreasing order of time – energy, distance and velocities. At 0 ns in Fig. 3 the hydrogen bond distance acfs of 2 water cluster relaxes later than the 6, 12 and 20 water molecule cluster. Here the 6, 12 and 20 water cluster relaxes within 0.2 ps but the 2 water cluster relaxes by 0.35 ps. Increasing the field effects the relaxation of water clusters. Relaxation times of different water clusters at different field strengths were analysed (with further details outlined in Supplementary Information), which draws essentially from an exp(−t/T) fit to each of the periodic VACF local peaks, described further in Refs. [40,41]. The relaxation in velocity auto-correlation functions (VACF) happened later than distance and energy and effect on relaxation with field was most pronounced in this quantity therefore it was analysed to estimate the relaxation times. For all the water clusters relaxation time increases with increase in field strength. For the 12 and 20 water cluster relaxation at 2.0 V/nm increased to almost twice that of relaxation in zero field intensities. It was also observed that at fields strengths of 0.01, 0.1 and 0.25 V/nm the relaxation time changes, further increase in field strengths increases the relaxation significantly. This has been reported earlier in a study by Futera and English and Avena et al.[42,43]. At high field intensities (>0.5 V/nm) acfs decorrelate by 0.3 ps which is somewhat higher than those at low field intensities. Energy autocoorelation functions relaxes much faster within 0.1 ps for all the water clusters and at all the fields. The behaviour of the 2 water cluster is different from the 6, 12 and 20 water cluster. In 2 water cluster the acfs uncorrelated later by 0.1 ps. The velocity autocorrelation function relaxes much later compared to the distance and energy correlation functions. Here the behaviour of the 2 water cluster is similar to the 6,12 and 20 water cluster. The

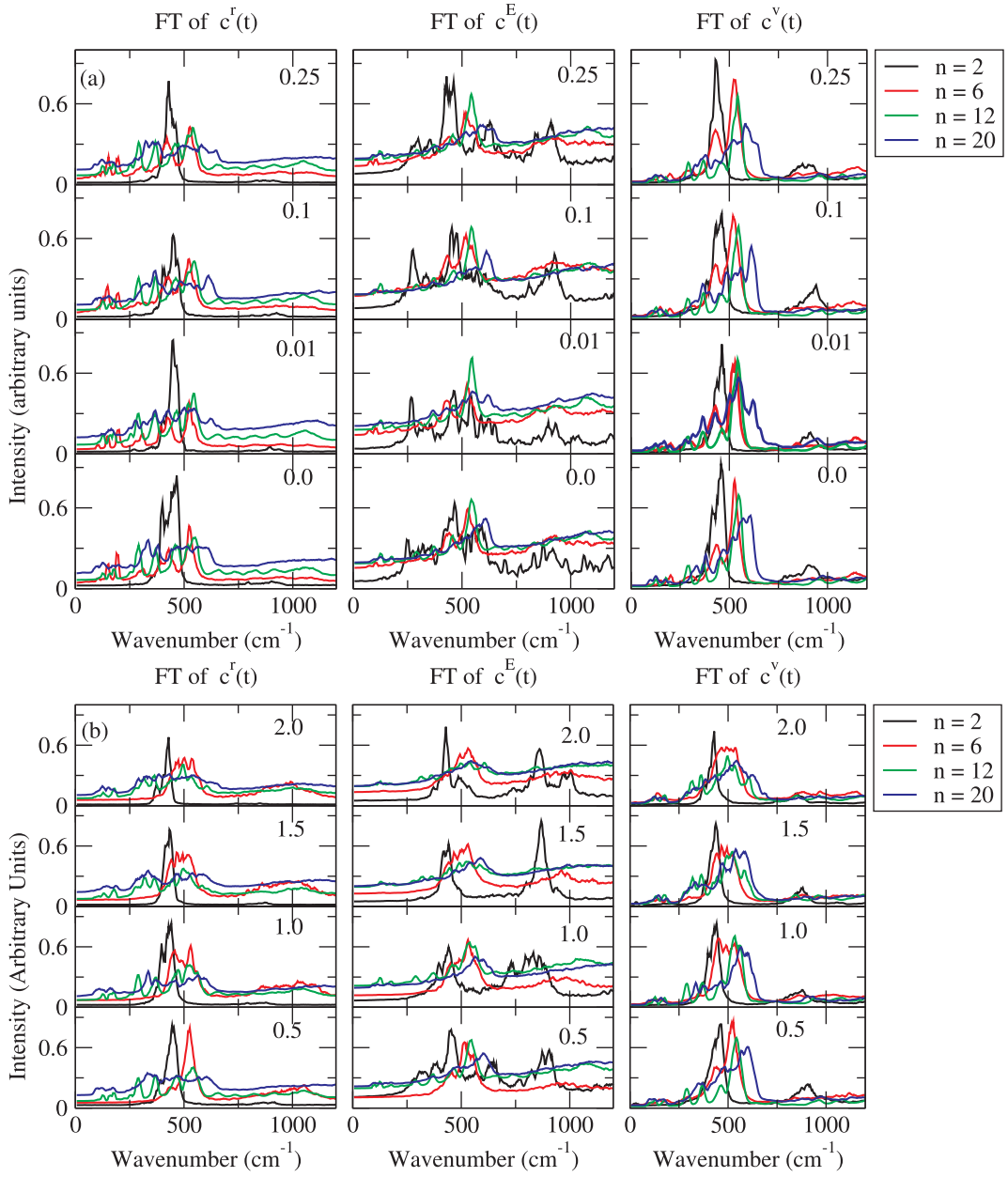

Fig. 7. (a) Fourier Transform of Autocorrelation functions at 800 ns at 0.0, 0.01, 0.1 and 0.25 V/nm. (b) Fourier Transform of Autocorrelation functions at 800 ns at 0.5, 1.0, 1.5 and 2.0 V/nm.

Table 4
Ratio of broken to original number of hydrogen bonds for different water clusters under varying field intesities.

Field strength (V/nm)	6	12	20
0.00	3/11	3/25	5/30
0.01	4/11	2/25	8/30
0.10	5/11	2/25	6/30
0.25	6/10	0/24	0/32
0.50	9/10	1/23	7/30
1.00	7/10	0/23	8/30
1.50	6/10	2/23	3/30
2.00	4/10	5/23	6/30

fluctuations in velocity acf remains in all the water clusters till 0.3 ps. The fluctutations are highest in the 2 water cluster.

At 800 ns in Fig. 5 acf plots are almost similar to the acfs at 0 ns under the influence of both low and high field intensities. The relaxation in all the quatities occur within 0.5 ps. Under all the electric field intensities the relaxation are alike. This is in spite of even less-intense fields leading to disruption and outright rupture of the original stabilising hydrogen bonds in each cluster, with re-formation into alternative structures. The relative similarity of the ACFs at the outset, and at later times signals that the distortion and twisting of hydrogen bonds occurs almost instantaneously (within less than 1 ns). Now, the intensity effect is interesting: careful scrutiny shows that the decay of the in-field ACFs slows with respect to the zero-field results with mounting field intensity, as the stronger static fields retard librational (rotation-oscillation) motion with suppressed scope for rotations and oscillation about hydrogen bonds (whether originally present from the zero-field-optimised starting point or distorted and rearranged rapidly in fields).

3.2. Spectra

Fourier transformations of acfs at 0 and 800 ns are plotted in Figs. 6 and 7. Fourier trasformations of acfs at 200, 400 and 600 ns were obtained but reported in Supplementary Material, because they were not significantly different from 0 and 800 ns. The above-mentioned suppression of rotational, and especially librational, motion is manifested somewhat dramatically with increasing field intensity by the reduction in prominence of the librational band (at 700–1200 cm^{-1} in the energy-spectra), together with a distinct red-shifting of the translational-optical spectra vis-a-vis zero-field conditions (at 400–600 cm^{-1} for the energy- and distance- spectra). This is especially true for the 20-water cluster, where the larger system-collective dipole allows a larger scope for field-induced dipolar realignment, and consequent hydrogen-bond rupture and strain. The induced dipolar alignment in static fields is correlated more with changes in energy- and distance- metrics, so these show a greater field effect than velocity spectra.

3.3. Hydrogen bond survival ratios

Hydrgen bond survival ratios were obtained for each of these water clusters. At each electric fields it was observed that the water structure distorts within 1 ns of the simulation. Table 4 shows the number of hydrogen bonds broken (numerator) in 6, 12 and 20 atom water cluster after 800 ns with respect to the original number of hydrogen bonds (denominator) in the cluster. Results were obtained after running a simulation of 1 ns after 800 ns. The hydrogen bonded neighbors' indices were matched at the beginning of 800 ns and at the end of 801 ns. It was observed that within few picoseconds of simulations cluster deforms and alternate hydrogen bonds are formed. This happens for all the water clusters under all the electric field intensities. It is observed that electric field strengths of magnitude till 2.0 V/nm does not completely break the hydrogen bonding arrangement as the number of broken hydrogen bonds is very few but deforms with respect to the original hydrogen bonded optimised structure. This is consistent with the earlier work where it was shown that water clusters adopt alternative hydrogen bonding arrangements in presence of electric fields [38]. With application of field the hydrogen bonds do not dissociate so to find new neighbors but deforms to retain the neighbors. This alternative hydrogen bond arrangement possibility is also reported in an earlier study of water octamer by Rojas et al.. Here they find that at high temperatures and low field strengths (1.0 V/nm) water octamers undergoes a 'solidlike' to 'liquidlike' transition and at low temperature water octamer undergoes a 'solidlike' to 'solidlike' at field strenghts >5 V/nm. Although our study focusses only on the effect of electric field strengths nevertheless hydrogen bonds taking alternate arragements with increase field strength is reported earlier and validates our findings [26].

4. Conclusion

The effect of varying field intensities on 2, 6, 12 and 20 water clusters are investigated here from Molecular Dynamics simulations. Water molecules were modeled using the TIP4P/2005 potential. Electric field intensities were varied from low 0.01 V/nm to high 2.0 V/nm. It was found that within 1 ns of the application of even less intense electric field the original hydrogen bond structure of the cluster deforms and finds alternate arrangement. The autocorrelation functions of velocity, energy and distance decays within few picoseconds almost irrespective of the field intensities. Power spectra analysis shows that overall the libration motion is most effected with the increase in field intensities. This is most pronounced in the 20 water cluster. Here librational motions are suppressed with the increase in the field intensities.

Acknowledgements

SNC would like to thank Sikkim University for providing the computational facilities to perform the simulations.

Appendix A. Supplementary material

Supplementary data associated with this article can be found, in the online version, at https://doi.org/10.1016/j.cplett.2018.08.061.

References

[1] F.H. Stillinger, Hydrogen-bond patterns in liquid water, Science 209 (1980) 451.
[2] N.J. English, Molecular dynamics simulations of liquid water using various long-range electrostatics techniques, Mol. Phys. 103 (2005) 1945.
[3] A. Luzar, D. Chandler, J. Chem. Phys. 98 (1993) 8160.
[4] S.N. Chakraborty, N.J. English, J. Chem. Phys. 143 (2015) 154504.
[5] G.S. Fanourgakis, E. Apra, S.S. Xantheas, High-level ab initio calculations for the four low-lying families of minima of (H2O)20. I. Estimates of MP2/CBS binding energies and comparison with empirical potentials, J. Chem. Phys. 121 (2004) 2655.
[6] K. Diri, E.M. Myshakin, K.D. Jordan, The role of vibrational anharmonicity on the binding energies of water clusters, J. Phys. Chem. 109 (2005) 4005.
[7] S. Bulusu, S. Yoo, E. Apra, S. Xantheas, X.C. Zeng, Lowest-energy structures of water clusters (H2O)11 and (H2O)13, J. Phys. Chem. A 110 (2006) 11781–11784.
[8] S. Yoo, E. Apra, X.C. Zeng, S.S. Xantheas, High-level ab-initio electronic structure calculations of water clusters (H2O)16 and (H2O)17: a new global minimum for (H2O)16, J. Phys. Chem. Lett. 1 (2010) 3122–3127.
[9] R. Torro, P. Bartolini, R. Righini, Nature 428 (2004) 296.
[10] N. Agmon, Acc. Chem. Res. 45 (2012) 63.
[11] Thomas D. Kühne, Rustam Z. Khaliullin, Electronic signature of the instantaneous asymmetry in the first coordination shell of liquid water, Nat. Comm. 4 (2013) 1450.
[12] J.R. Errington, P. Debenedetti, Nature 409 (2001) 318.
[13] D. Laage, J.T. Hynes, Science 311 (2006) 832.
[14] Soohaeng Yoo, Mikhail V. Kirov, Sotiris S. Xantheas, Low-energy networks of the T-Cage (H2O)24 cluster and their use in constructing periodic unit cells of the structure I (sI) hydrate lattice, J. Am. Chem. Soc. 131 (2009) 7564–7566.
[15] N.J. English, C.J. Waldron, Perspectives on external electric fields in molecular simulation: progress, prospects and challenges, PhysChemChemPhys 17 (2015) 12407–12440.
[16] Tim James, David J. Wales, J. Chem. Phys. 126 (2007) 054506.
[17] Glen L. Holden, David L. Freeman, J. Chem. Phys. B 115 (2011) 4725.
[18] Andrei V. Egorov, Elena N. Brodskaya, Aatto Laaksonen, Mol. Phys. 100 (2002) 941.
[19] http://www.gromacs.org.
[20] M. Yoshida, K. Kikuchi, T. Maekawa, H. Watanabe, J. Phys. Chem. 96 (1992) 2365–2371.
[21] P. Poulain, R. Antoine, M. Broyer, P. Dugourd, Chem. Phys. Lett. 401 (2005) 1–6.
[22] F. Calvo, P. Dugourd, Biophys. J. 95 (2008) 18–32.
[23] F. Manca, S. Giordano, P.L. Palla, F. Cleri, L. Colombo, J. Chem. Phys. 137 (2012) 244907.
[24] Y.C. Choi, C. Pak, K.S. Kim, J. Chem. Phys. 124 (2006) 094308.
[25] C.E. Dykstra, Chem. Phys. Lett. 299 (1999) 132.
[26] J. Hernndez-Rojas, B.S. Gonzlez, T. James, D.J. Wales, J. Chem. Phys. 125 (2006) 224302.
[27] D. Rai, A.D. Kulkarni, S.P. Geiji, R.K. Pathak, J. Chem. Phys. 128 (2008) 034310.
[28] E.J.L. Toledo, R. Custodio, T.C. Ranalho, M. Eugenia, G. Porto, Z.M. Magriotis, J. Mol. Struct. Theochem. 915 (2009) 170.
[29] M. Karahka, J. Kreuzer, Phys. Chem. Chem. Phys. 13 (2011) 11027.
[30] D. Rai, A.D. Kulkarni, S.P. Geiji, R.K. Pathak, J. Chem. Phys. 135 (2011) 024307.
[31] S. Acosta-Gutiuez, J. Hernndez-Rojas, J. Bretn, J.M. Gomez Lorente, D.J. Wales, J. Chem. Phys. 135 (2011) 124303.
[32] D. Rai, A.D. Kulkarni, S.P. Geiji, L.J. Bartolotti, R.K. Pathak, J. Chem. Phys. 138 (2013) 044304.
[33] A. Modal, H. Seenivasan, S. Saurav, A.K. Tiwari, Indian J. Chem. 52A (2013) 1056–1060.
[34] P. Gallo, et al., Chem. Rev. 116 (2016) 7463–7500.
[35] I.M. Svishchev, P.G. Kusalik, Phys. Rev. Lett. 73 (1994) 975.
[36] P.K. Nandi, C.J. Burnham, N.J. English, Phys. Chem. Chem. Phys. 20 (2018) 8042–8053.
[37] J.L.F. Abascal, C. Vega, J. Chem. Phys. 123 (2005) 234505.
[38] Tim James, David J. Wales, Javier Hernandez-Rojas, Chem. Phys. Lett. 415 (2005) 302.
[39] http://www-wales.ch.cam.ac.uk/wales/CCD/TIP4P-water.html.
[40] N.J. English, J.S. Tse, D. Carey, Phys. Rev. B. 80 (13) (2009) 134306.
[41] N.J. English, J.S. Tse, Phys. Rev. Lett. 103 (1) (2009) 015901.
[42] Zdenek Futera, Niall J. English, J Chem. Phys. 147 (2017) 031102.
[43] M. Avena, P. Marracino, M. Liberti, F. Apollonio, N.J. English, J. Chem. Phys. 142 (14) (2015) 141101.